Int. J. Nanoelectronics and Materials **2 No.1** (2009) 23-39

Estimation of thermal contact resistance in metal-plastic interface of semiconducting electronic devices

S. A. Oke[1,*], A. A. Oyekunle[1], T. A. O. Salau[2], A. A. Adegbemile[3], K. O. Lawal[3]

[1,2)] *Department of Mechanical Engineering, University of Lagos, Nigeria.*
[2)] *Department of Mechanical Engineering, University of Ibadan, Nigeria.*
[3)] *Faculty of Engineering, University of Ado-Ekiti, Nigeria.*

Abstract

For decade, thermal contact resistance (TCR) has been measured experimentally. Unfortunately, the database, which should regularly support decision-making on TCR coefficients, seems not to exist. Thus, companies result to using outdated or irrelevant data that limits lifespan of electronics devices, their performance and reliability. This paper mathematically models the problem of TCR between two media (plastic-metal interface) in semi conductors with reference to resistance and the flow of heat across or interface of two surfaces that are in contact, particularly in engineering applications. In this paper, a semi-conductor/heat sink assembly is used to model the behaviour of thermal contact resistance. A cylindrical shaped semi-conductor was conceptualised, with the governing differential equations derived and the boundary conditions for the problem stated. The effect of parameters such as surface roughness, contact pressure, density of interstitial gas, heat capacity, thermal and mechanical properties on the temperature at the center of the semi-conductor was studied. From the analysis, it can be inferred that by effectively lowering thermal contact resistance, efficient heat transfer results, which helps to prolong the life and reliability of the semi-conductor. The current work is motivated to fill an important gap that may be beneficial to practitioners in the semi-conductor industry.

Keywords: Thermal, Resistance, Plastics, Performance, Electronic devices.

1. Introduction

Effective description of thermal energy is a necessary and important aspect in the electronic industry. In order to increase the performance, reliability and life span of an electronic device, the efficient removal of heat from the device to the atmospheric environment is very important. This concept is referred to as the thermal energy transfer (TET). The thermal energy transfer (removal) involves the following stages: (a) The volumetric heat generation within the device; (b) The transfer of heat from the semi-conducting device to the heat sink; (c) The heat transfer from the heat sink to the

[*]) For correspondence, E-mail: sa_oke@yahoo.com

environment (Rajput, 1998; Yang, 2007; MIT, 2007). We are most concerned with (b), that is, the efficient transfer of heat from the semi-conducting device to the heat sink.

Now, consider the semi-conducting device/heat sink assembly, in place of air, which fills up the interstitial spaces between the two non-conforming surfaces, there are some applications where materials of higher thermal conductivity known as thermal interface material, are used. With the use of thermal interface materials, there are two possibilities: (1) the thermal interface material fills up the gaps within the interface such that there are still contacts between the two surfaces at some points. Thus, in the circuit, the resistance is replaced with the estimated thermal resistance of the thermal interface material; (2) the thermal interface material could be such that it completely separates the two surfaces, filling the gaps between them (Rajput, 1998; MIT, 2007).

From the foregoing, it is important to define the problem solved in this paper. This is stated as follows:

> *"In a semiconductor device (i.e. field effect transistor), the heat is generated in the channel and conducted to the chip on the silicon substrate. The heat is removed from the chip to the environment by appropriate packaging techniques. Typically, semiconductor electronics and packaging problems involve planar structures (chip, package, boards, etc). This problem is of importance to researchers in thermal contact resistance."*

Thus, the problem is approached by considering a semi-conductor/heat sink assembly and modelling the behaviour of the thermal contact resistance. A cylindrical-shaped conductor is used for the modelling. This is formulated as a problem and an appropriate solution methodology sought for.

The following is a review of related studies on thermal contact resistance: Barber (1986) studied the effect of mechanism on the axial temperature variation in parallel or counter flow heat exchangers. A method was developed for integrating the controlling equations for an arbitrary, non-linear, pressure-dependent contact resistance without iteration and the effect of prestress and other parameters on the occurrence of multiple solutions is discussed. Cong et al. (2006) carried out numerical simulation of both the three-dimensional heat conduction and two-dimensional elastic wave propagation at the interface of contact solids. Numerical results of heat conduction simulations show that both the true contact area and thermal contact conductance increase linearly with an increase in the contact pressure.

Yang (2007) applied a conjugate gradient method based on an inverse algorithm to estimate the unknown time-dependent 'thermal contact resistance' in a single-coated optical fiber, which is subjected to transient 'thermal' loading. Vermeersch and DeMercy (2007) numerically calculated the 'thermal' impedance/ $z_{th}(j\omega)$ for a silicon chip glued on a ceramic substrate by modelling the chip-substrate interface as a 'thermal contact resistance' (γ_c). In the investigation by McDonald, et al. (2007) plasma-sprayed molybdenum and ythia-stabilized zirconia particles (38-63μ diameters) were sprayed onto glass and Inconnel 625 held at either room temperature and 400^{o}C samples of Inconnel 625 were preheated for 3h, and then air-cooled to room temperature before spraying. Photographs of the splats were captured using a fast charge–coupled device (CCD) camera. A rapid two-color pyrometer was used to collect "thermal radiation from the particles during flight and spreading to follow the evolution of their temperature. The temperature evolution was used to determine the cooling rate of spreading particles. An analytical heat conduction model was developed to calculate the 'thermal contact resistance' at the interface of the plasma-sprayed particles and the surfaces from splat cooling rates.

Shinji et al. (2005) proposed the quantitative measuring method of the thermal contact resistance in consideration of the real contact area of the joint and make clear its validity and the possibility of formulation of the resistance. Bahrami et al. (2004) developed a compact analytical model for predicting thermal contact resistance of non conforming rough contacts of bare solids in a vacuum by employing the 'Scale analysis method'. It is demonstrated that the geometry of heat sources on a half-space for micro contacts is justifiable for applicable range of contact pressure. Bahrami et al. (2005) developed a new model which is for low pressures. The effect of elastications beneath the plastically deformed micro contacts is determined by superimposing normal deformations due to self and neighboring contact spots in an elastic half space. Muzuhara and Ozawa (1999) examined an estimation method of the titled resistance value in the contact surface between objects. The paper showed the composition of a measuring device and a measurement method of both resistance, and measurements were conducted for lapped surface, ground surface and scraper surface of cast iron. Cook et al. (1984) presented a novel concept for reducing thermal contact resistance. Gavarella et al. (2003) considered an idealized problem, which a thermo elastic rod slides against a rigid plane with both frictional heating and a contact resistance. From the foregoing review, it seems obvious that investigations relating to the inclusion of diverse parameters in thermal contact resistance studies appear lacking in the literature. The need to close this important gap has therefore motivated the current work.

The structure of the paper is as follows: introduction, mathematical framework, results and discussion, and conclusion. The introduction provides the motivation for the study and a justification for the approach utilised in the current work by pointing out the gap in the literature. The problem definition is also included in this section. The problem is defined in order to have a clear focus of the challenge faced in concise form. The mathematical framework is commenced by stating the nomenclature and then the problem. It models the problem in a practically acceptable form. The section on mathematical framework also considers the problem analysis and the application of dimensional analysis in solving the problem. Results are displayed in the next section. The last section contains the concluding remarks.

2. Mathematical framework

2.1 Definition of terms

q_g uniform volumetric heat generation per unit volume per unit time
Q_g volumetric heat source in device. We assume a value of $10W/m^3$
A surface area of contact. We assume a cylinder of length 3cm and radius 0.5cm and we have chosen $1/12^{th}$ of the whole body for our analysis since there is symmetry.
T surface temperature
T_a ambient temperature (Temperature of the environment chosen as 23^oC)
H convective heat transfer coefficient of air. We assume natural convection and a value of $h = 30W/m^2k$
T_{max} the temperature at the center of the semi-conductor, the maximum temperatures
T_s the temperature at the outer surface at the heat sink
R_1 thermal resistance of the semi-conductor
R_a thermal resistance of the interstitial gas
R_2 thermal resistance of the heat sink
R_m thermal resistance of interface material
P pressure
σ surface roughness

ρ density of interstitial gas
μ viscosity
c_p heat capacity
k thermal conductivity
T temperature
V velocity (of interstitial gas)
k_1 thermal conductivity of semi-conducting device. We assume a value of 60Wm/k
k_2 thermal conductivity of heat sink. We assume a value of 250Wm/k
x the thickness of the interface between semi-conducting device/heat, assumed as 10μm
k_a thermal conductivity of air = 0.13W/mk
A_g gap heat transfer area
D a dimensionless parameter which should be a property of the fluid (air). The Prandtl number is one of the dimensionless parameter we expect to have effect on D.

2.2 Problems analysis

At the interface of the semi-conducting device and heat sink, there exists a phenomenon known as thermal contact resistance (TCR). Thermal contact resistance is a resistance to the flow of heat across an interface of two surfaces that are in contact. An illustration is shown in Figure 1. The contacting surfaces of the semi-conducting device and heat sink are not perfectly smooth. Therefore, the real contact area is less than the nominal contact area. Below are some of the factors considered which may influence the value of thermal contact resistance.

(i) *Contact/Bearing Pressure*: It is reasoned that as the contact pressure between the two surfaces increases, heat transfer becomes more efficient and thermal contact resistance is reduced.
(ii) *Deformation*: Preceding from (i) above, that if it is possible to deform the two materials up to an extent where the thermal properties are not too affected, actual surface area of contact can be increased thereby reducing thermal contact resistance.
(iii) *Nature of gap materials*: Since we have established that the two surfaces in contact are not perfectly smooth, the gaps or voids between the mating surfaces will be filled with some sort of gases or fluids (since we are not expecting there to be a vacuums). For the purpose of this paper, we will take air as the material filling up these gaps. The pressure of air within the mating surfaces and its thermal properties will have effect on the TCR.
(iv) *RMS value* σ: We shall also take a look at the quantity rms which is used as a measure of the roughness of a surface.
(v) *Temperature of the interstitial material*: There is possibility of higher temperatures of interstitial material increasing the rate of heat transfer. Since with higher temperature, the gas particles will collide more often.

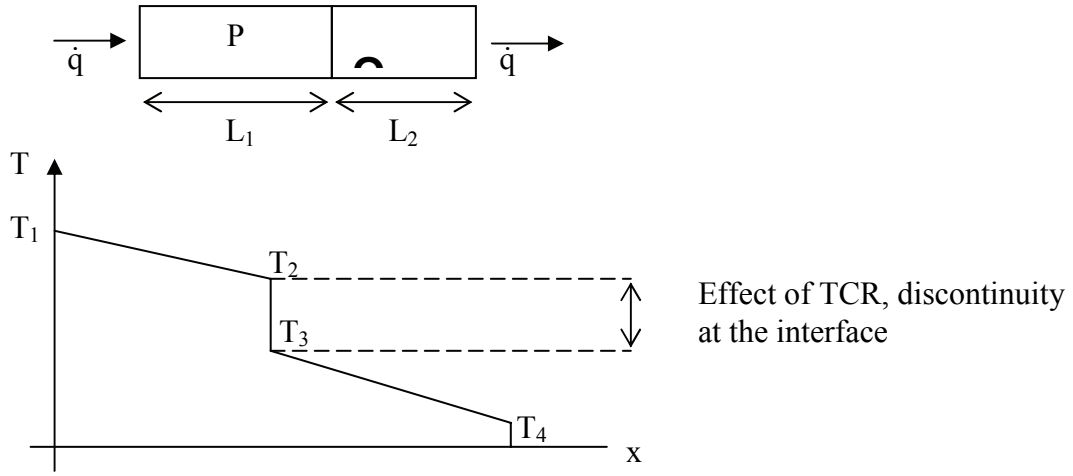

Fig. 1: Illustrating the phenomenon of thermal contact resistance.

Without the effect of TCR, we would expect the temperature gradient to be like that illustrated in Figure 2.

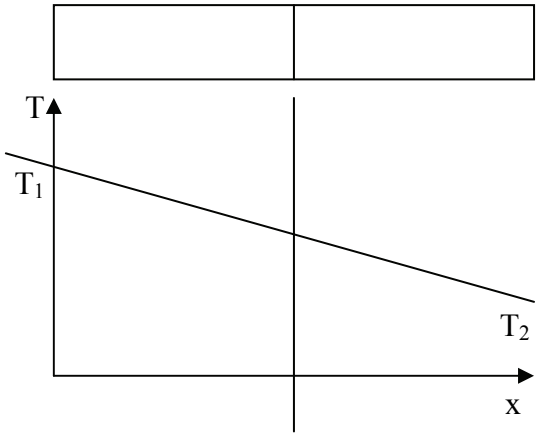

Fig. 2: Temperature gradient in thermal contact resistance system.

For the sake of simplicity, the semi-conducting device is modeled as a cylinder shape, which generates uniform volumetric heat from within. The semi-conducting device is modeled as shown in Figure 3 while the heat sink as shown in Figure 4.

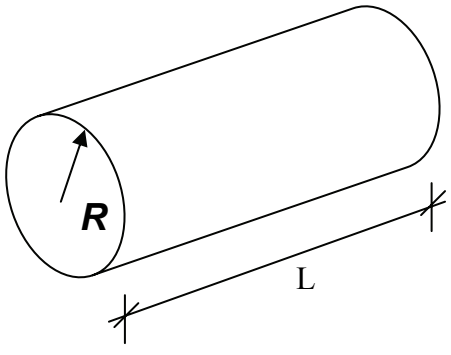

Fig. 3: Cylinder of length L and radius R.

On a 2-D plane, the semi-conducting device and the heat sink together can be imagined to understand its structure. Since the whole assembly is symmetrical, we can pick a part of it, write the governing equations and apply them to the whole of the body.

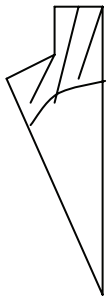

Fig. 4: Elemental part of semi-conducting device and heat sink.

Derivation of governing equation

From first principle, we have

$$\nabla.\,(k\nabla T) + q_g = \rho c_p \frac{dT}{dt}, \text{ where } \nabla \text{ is defined as } \frac{\partial}{\partial x_i} \tag{1}$$

For a constant k, (i) becomes:

$$\nabla^2 T + \frac{q_g}{k} = \rho \frac{c_p}{k} . \frac{dT}{dt} \tag{2}$$

For the steady state situation, we are considering, the right hand side value becomes zero in equation (2),

$$\nabla^2 T + \frac{q_g}{k} = 0 \text{ . Thus, we have } \frac{\partial^2 T}{\partial x^2} + \frac{\partial^2 T}{\partial y^2} + \frac{\partial^2 T}{\partial z^2} + \frac{q_g}{k} = 0 \tag{3}$$

For a one-dimensional heat transfer, equation (iii) is reduced to: $\frac{\partial^2 T}{\partial x^2} + \frac{q_g}{k} = 0$

Heat transfer from heat generated within volume to the interface (Figure 5) from Fourier's law,

$$Q = - KA \frac{dT}{dx} \tag{4}$$

Considering an elemental strip of the cylinder with radius r and thickness dr,

$$Q_r = -K2\pi rL.\ \frac{dT}{dr} \tag{5}$$

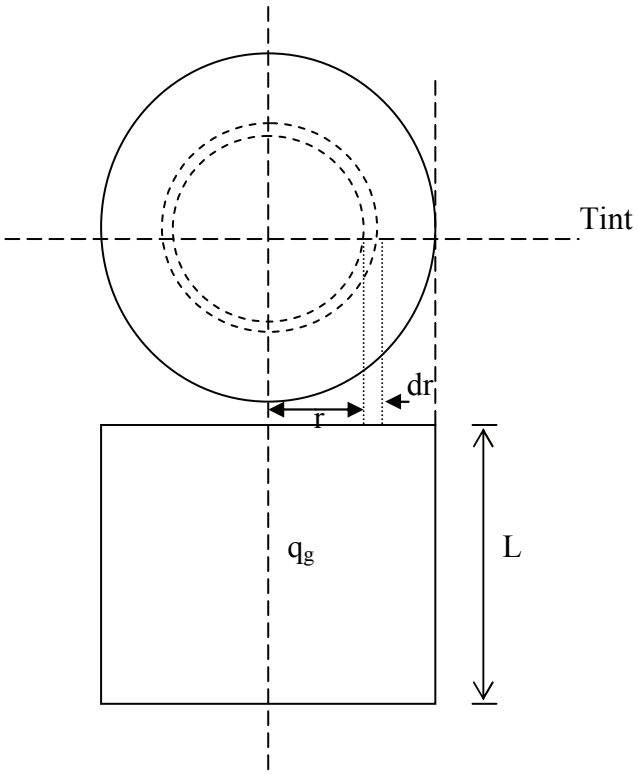

Fig. 5: Heat generation profile.

But $A = 2\pi rL$, therefore heat generated in the element $Q_g = q_g \times$ volume

$$Q_g = q_g \times (\text{Area}) \times L = q_g \times (2\pi r.dr) \times L = q_g\ .\ (2\pi rdr).L \tag{6}$$

Heat out at radius r + dr is derived from $Q(r + dr) = Qr + \frac{d}{dr}(Qr)\ dr$

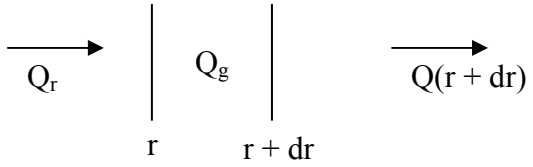

For energy balance, $Q_r + Q_g = Q(r + dr)$. Therefore

$$Q_g = \frac{d}{dr}\ (Q_r)\ dr \tag{7}$$

By substituting (5) and (6) into (7), we have

$$q_g \,.\, 2\pi r.dr.L = \frac{d}{dr}\left[-k\,.\,2\pi rL.\frac{dT}{dr}\right]dr \text{ or } \frac{d}{dr}\left[r\,.\,\frac{dT}{dr}\right] = -\frac{q_g r}{k}$$

By integrating, $r\frac{dT}{dr} = -\frac{q_g r^2}{k^2} + a$. This means

$$\frac{dT}{dr} = -\frac{q_g}{k}\frac{r}{2} + \frac{a}{r} \tag{8}$$

Integrating (8): $T = -\frac{q_g}{k}\frac{r^2}{4} + a\ln r + b$ (8a)

The constants a and b can be evaluated from the boundary conditions as follows:

(1) at r = R, $T = T_{int}$, and (2) $q_g(\pi R^2 L) = -K\,.\,2\pi RL\,.\left[\frac{dT}{dr}\right]_{r=R}$ (9)

At r = 0, $\frac{dT}{dr} = 0$. From (8), $\left(\frac{dT}{dr}\right)_{r=R} = -\frac{q_g}{k}\frac{R}{2} + \frac{a}{R}$. Also, From (2), $\left(\frac{dT}{dr}\right)_{r=R} = -\frac{q_g}{k}\frac{R}{2}$.

Then, equating both terms, it is clearly seen that a = 0. Therefore, $T_{int} = -\frac{q_g}{k}\frac{R^2}{4} + b$, and

$b = T_{int} + -\frac{q_g}{k}\frac{R^2}{4}$. By substituting values of a and b in (8a):

$$T = -\frac{q_g}{k}\frac{R^2}{4} + T_{int} + -\frac{q_g}{k}\frac{R^2}{4} = T_{int} + \frac{q_g}{4k}(R^2 - r^2) = T_{int} + \frac{q_g}{4k}R^2\left(1 - \frac{r^2}{R^2}\right)$$

In terms of dimensionless parameters,

$$\frac{T - T_{int}}{\frac{q_g R^2}{4k}} = 1 - \frac{r^2}{R^2} \tag{10}$$

If we plot equation (10) on a graph, we get a parabolic curve as shown below:

$$\frac{T - T_s}{\frac{q_g R^2}{4k}}$$

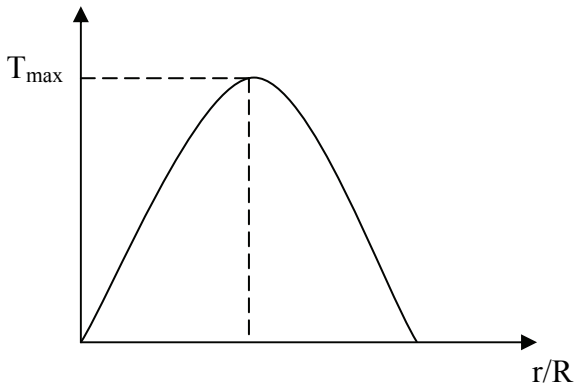

Fig. 6: Parabolic shape of curve of parameters.

T_{max} occurs at r = 0 (Figure 6). Our aim is now to limit T_{max} to the level that will not cause damage to the semi-conducting device.

$$T_{max} = Tint + \frac{q_g}{4k} . R^2 \qquad (11)$$

At the interface, there is a jump or slip in time, which is due to thermal contact resistance. Let us represent this jump or slip by ΔT_{int}. Using the electrical circuit analogy, we can draw our circuit as shown in Figure 7:

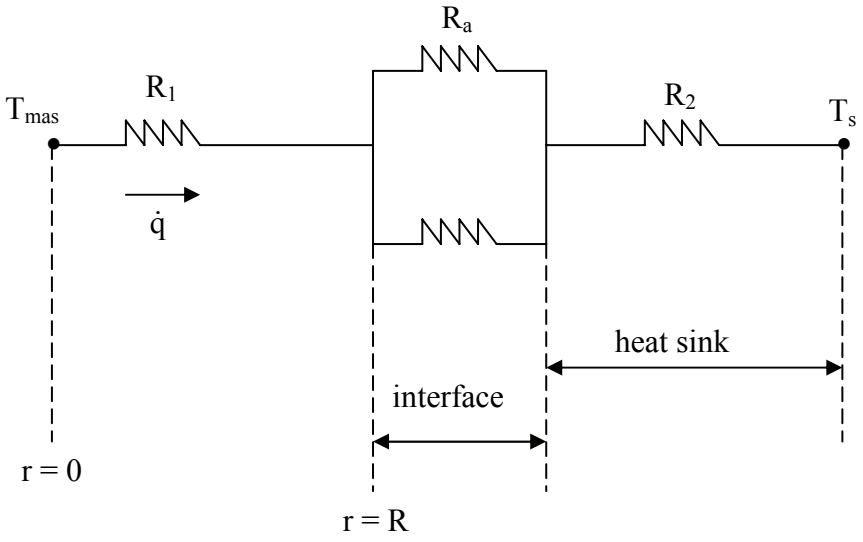

Fig. 7: Circuit diagram for the system under study.

We have

$$q = \frac{T_{max} - Ts}{\Sigma R_T} \tag{12}$$

But $$\Sigma R_T = R_1 + \left(\frac{1}{R_a} + \frac{1}{R_{cr}}\right)^{-1} + R_2 \tag{13}$$

Therefore $$q = \frac{\Delta T\,int}{\left(\frac{1}{R_a} + \frac{1}{R_{cr}}\right)^{-1}} \tag{14}$$

Note that in this work, interstitial gas is assumed to be air.

2.2.1 Dimensional analysis

With the use of Buckingham π theorem, we want to try to derive dimensionless parameters that may affect the thermal contact resistance.
Supposing the thermal contact resistance depends on the following parameters:

Parameters	***Dimensions***
Pressure, P	$ML^{-1}T^{-2}$
Surface roughness, σ	L
Density of interstitial gas, ρ	ML^{-3}
Viscosity, μ	$ML\text{-}^{1}T^{-1}$
Heat capacity, c_p	$L2T^{-2}\theta^{-1}$
Thermal conductivity, k	$MLT\text{-}3\theta^{-1}$
Temperature, T	θ
Velocity, V (of interstitial gas)	$M^{-1}L^{-2}T^{3}\theta$

Note that $R_{cr} = f(P, \sigma, \rho, \mu, c_p, k, T, v)$. Then, we could state that $f(R_{cr}, P, \sigma, \rho, \mu, c_p, k, T, v) = 0$. Then $f(\pi_1, \pi_2, \pi_3, \pi_4, \pi_5) = 0$

$$\pi_1 = T^{a1} . \sigma^{b1} . \rho^{c1} . V^{d1} . P$$
$$\pi_2 = T^{a2} . \sigma^{b2} . \rho^{c2} . V^{d2} . P$$
$$\pi_3 = T^{a3} . \sigma^{b3} . \rho^{c3} . V^{d3} . P$$
$$\pi_4 = T^{a4} . \sigma^{b4} . \rho^{c4} . V^{d4} . P$$
$$\pi_5 = T^{a5} . \sigma^{b5} . \rho^{c5} . V^{d5} . P$$

T, σ, ρ, v have been chosen as our repeating variable.

By solving the π-term, we obtain: $\pi_1 = \frac{p}{\rho v^2}$, $\pi_2 = \frac{\rho v \sigma}{\mu}$, $\pi_3 = \frac{kT}{\rho v^3 \sigma}$, $\pi_4 = R_{cr}\frac{\rho v^3 \sigma^2}{T}$, and $\pi_5 = \frac{c_p T}{v^2}$. Note that π_2 gives us the Reynold's coefficient, and combination of π_2, π_3 and π_5 gives $\frac{k}{\mu c_p}$, which is Prandth number, which is a property of the fluid.

By referring to our problem model, we have the following (Figure 8)
:

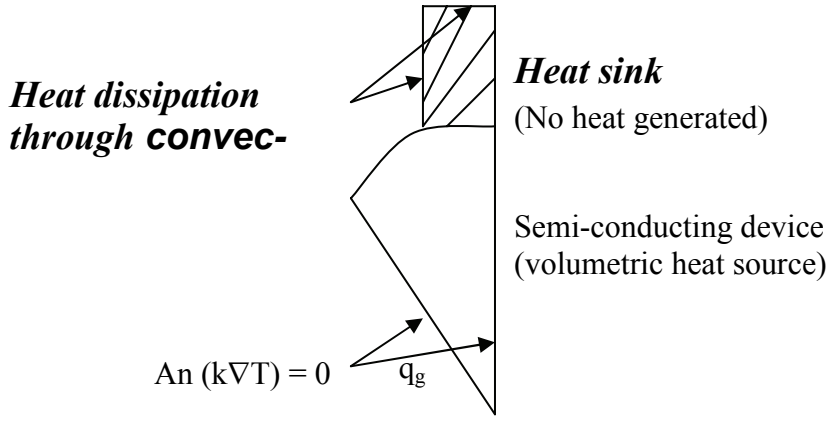

Fig. 8: Detailed diagram of semi-conducting device and heat sink.

Using the series analogy of heat transfer, we model k_c (thermal conductivity at points of contact in the interface) as:

$$\frac{1}{k_c} = \frac{1}{k_1} + \frac{1}{k_2} = \frac{k_1 + k_2}{k_1 k_2}. \text{ Note that } k_c = \frac{k_1 k_2}{k_1 + k_2} \tag{15}$$

We assume effective surface roughness σ as 15μm, we can now write

$$R_{cr} = \left(\frac{\sigma}{k_1 An}\right) c \tag{16}$$

where c would be a dimensionless parameter which would be a constant for any particular semi-conducting device.

3. Results and discussion

To bring in the effect of the contact/bearing pressure mentioned in the earlier part of this work, we are more inclined to pick c as $\frac{p}{\rho v^2}$. Density of air ρ = 1.3kg/m3 If we assume

P = 2Pa and v = 2m/s, c = $\frac{p}{\rho v^2} = \frac{2}{1.3\times 2^2} = 0.385$. From (15), kc = $\frac{60\times 250}{60+250} = \frac{15000}{310} =$ 48.39Wm/k.

We model thermal resistance of air R_a as: $\left(\frac{x}{k_a Ag}\right)^D$

$$A = \frac{1}{6}\pi RL = \frac{1}{6} \times \frac{22}{7} \times 0.5 \times 3 \times 10^{-4} = 0.79 \times 10^{-4} m^2$$

Let D = 0.007, then $R_a = \left(\frac{10\times 10^{-6}}{0.13\times 0.79\times 10^{-4}}\right)^{0.007} = 6.82 \times 10^{-3}$k/w, and

$R_{cr} = \left(\frac{1.5\times 10^{-6}}{48.39\times 0.5\times 10^{-4}}\right)^{0.385} = 2.39\ 10^{-4}$k/w

Going back to Figure 8, the values could be indicated on the assembly as follows:

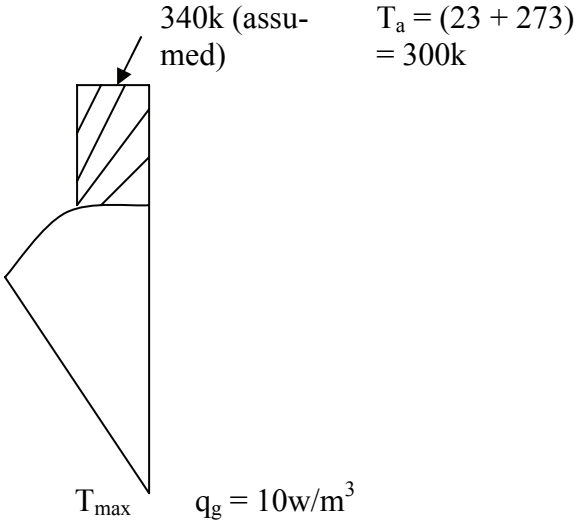

Fig. 9: Part of the semi-conducting device with specification.

With the combination of equations (xii), (xiii) and (xiv), a lower value of T_{max} is obtained when the value of R_{cr} is not considered. The following results are then obtained from the simulated data used for the work (Tables 1 and 2).

σ(μm)	m	F(N)	S(MN/m)	$A_0(m^2)$	x(μm)	y(μm)	b(μm)	$A_r(m^2)$	$P(N/m^2)$	$H(N/m^2)$	k(W/mk)	Rc(k/W)
5	0.2	200	500000	0.0025	0.0004	4.9996	0.002	1.257E-17	80000	2000000	230	3.452536
5	0.2	250	500000	0.0025	0.0005	4.9995	0.0025	1.964E-17	100000	2000000	230	2.760651
5	0.2	300	500000	0.0025	0.0006	4.9994	0.003	2.828E-17	120000	2000000	230	2.299395
5	0.2	350	500000	0.0025	0.0007	4.9993	0.0035	3.849E-17	140000	2000000	230	1.969928
5	0.2	400	500000	0.0025	0.0008	4.9992	0.004	5.027E-17	160000	2000000	230	1.722828
5	0.2	450	500000	0.0025	0.0009	4.9991	0.0045	6.363E-17	180000	2000000	230	1.53064
5	0.2	500	500000	0.0025	0.001	4.999	0.005	7.855E-17	200000	2000000	230	1.376891
5	0.2	550	500000	0.0025	0.0011	4.9989	0.0055	9.505E-17	220000	2000000	230	1.251096
5	0.2	600	500000	0.0025	0.0012	4.9988	0.006	1.131E-16	240000	2000000	230	1.146268
5	0.2	650	500000	0.0025	0.0013	4.9987	0.0065	1.327E-16	260000	2000000	230	1.057568
5	0.2	700	500000	0.0025	0.0014	4.9986	0.007	1.54E-16	280000	2000000	230	0.981539
5	0.2	750	500000	0.0025	0.0015	4.9985	0.0075	1.767E-16	300000	2000000	230	0.915648
5	0.2	800	500000	0.0025	0.0016	4.9984	0.008	2.011E-16	320000	2000000	230	0.857994
5	0.2	850	500000	0.0025	0.0017	4.9983	0.0085	2.27E-16	340000	2000000	230	0.807123
5	0.2	900	500000	0.0025	0.0018	4.9982	0.009	2.545E-16	360000	2000000	230	0.761905
5	0.2	950	500000	0.0025	0.0019	4.9981	0.0095	2.836E-16	380000	2000000	230	0.721447
5	0.2	1000	500000	0.0025	0.002	4.998	0.01	3.142E-16	400000	2000000	230	0.685035

Table 1: Simulated data of various parameters of the model.

F(N)	n	$nA_r(m^2)$
200	7.95672E+12	0.0001
250	6.36537E+12	0.000125
300	5.30448E+12	0.00015
350	4.54669E+12	0.000175
400	3.97836E+12	0.0002
450	3.53632E+12	0.000225
500	3.18269E+12	0.00025
550	2.89335E+12	0.000275
600	2.65224E+12	0.0003
650	2.44822E+12	0.000325
700	2.27335E+12	0.00035
750	2.12179E+12	0.000375
800	1.98918E+12	0.0004
850	1.87217E+12	0.000425
900	1.76816E+12	0.00045
950	1.6751E+12	0.000475
1000	1.59134E+12	0.0005

Table 2: Simulated values of F(N) against $nA_r(m^2)$.

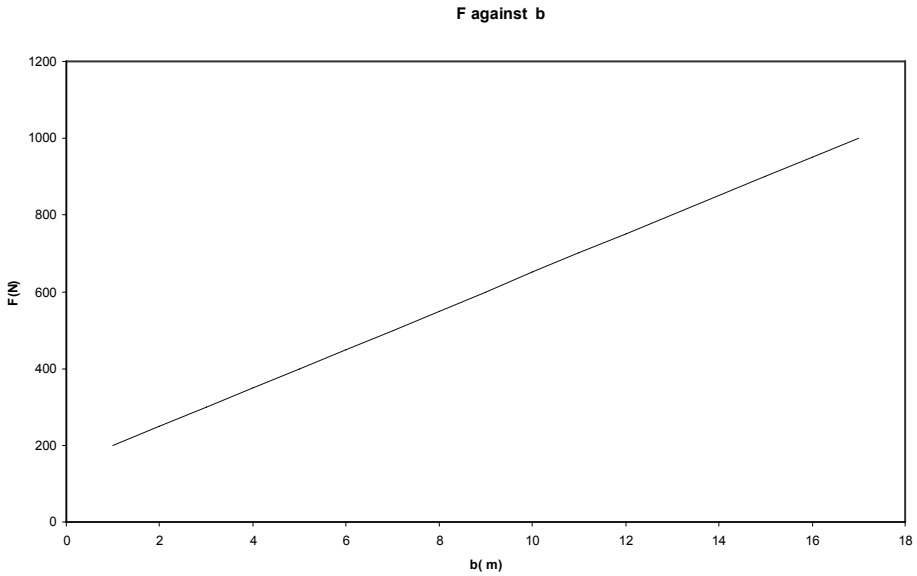

Fig. 10: Plotted values of F and b.

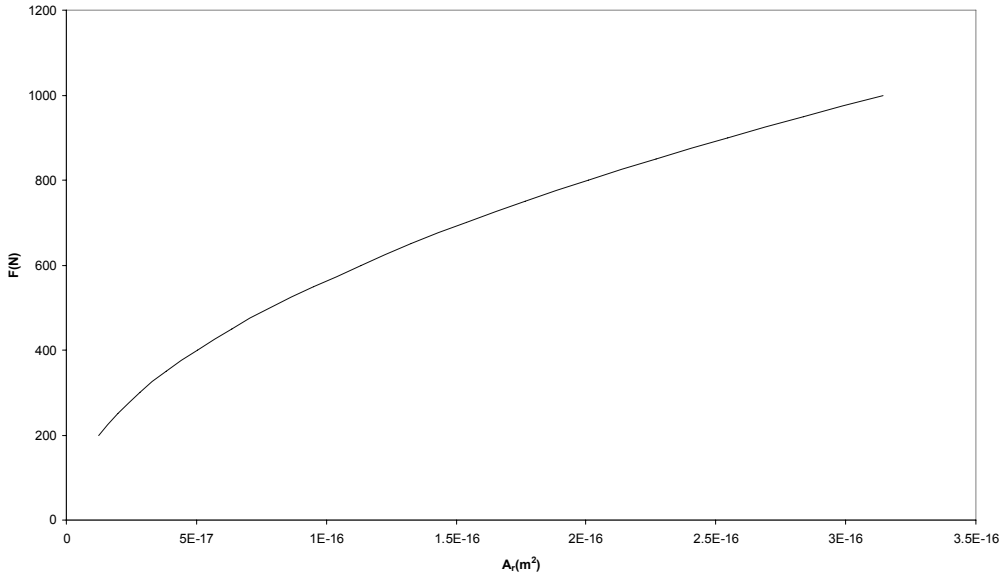

Fig. 11: Plotted values of F and A_T.

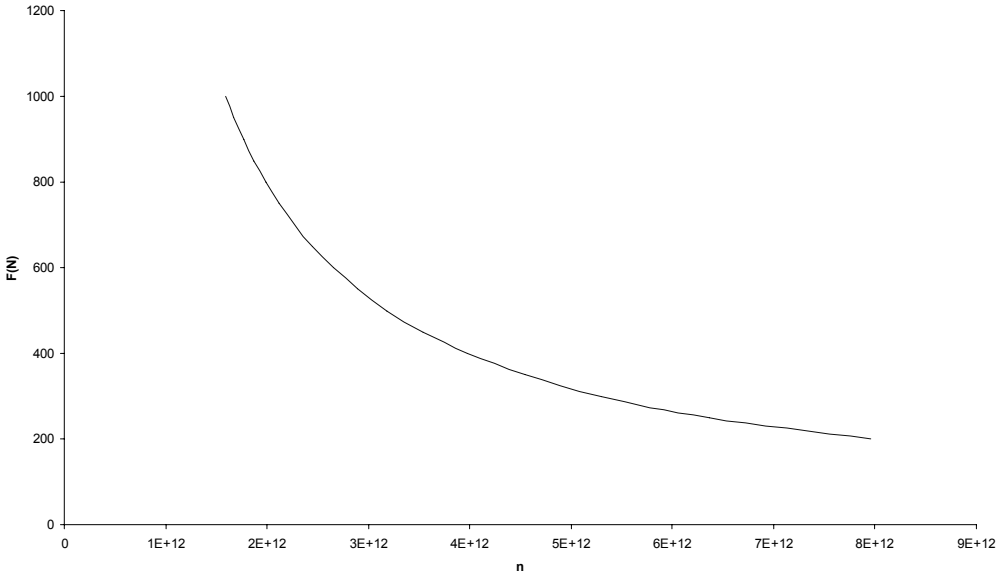

Fig. 12: Plotted values of F and n.

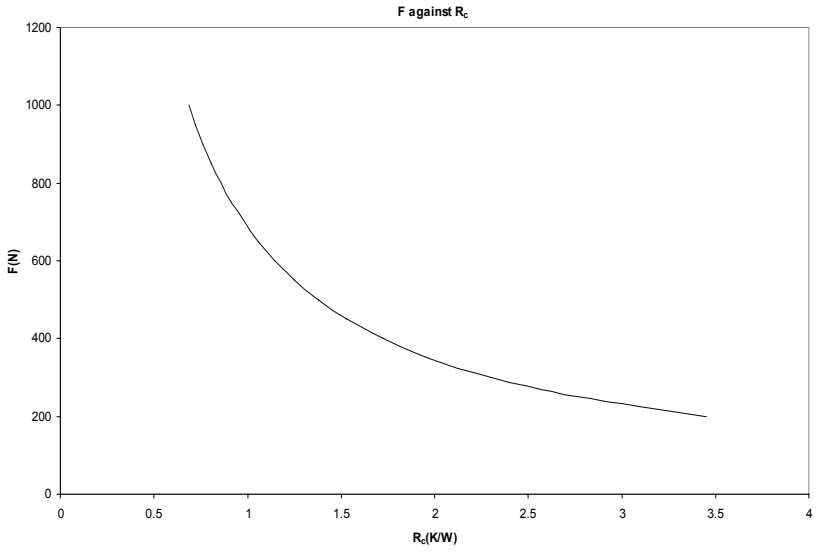

Fig. 13: Plotted values of F and R_c.

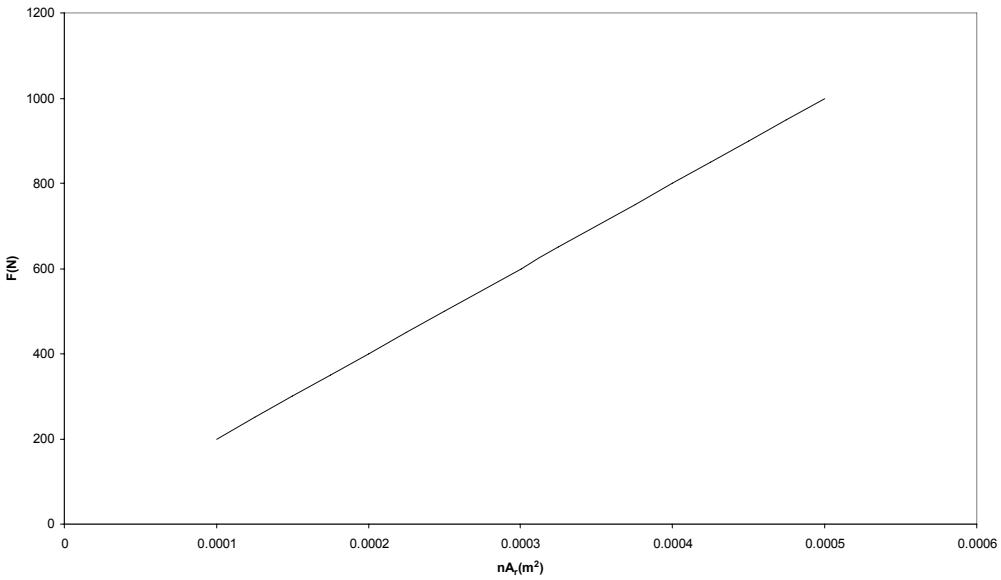

Fig. 14: Plotted values of F and nA_T.

4. Conclusion

In the present paper, we have investigated the interaction among the parameters of thermal contact resistance that is suspected to have effects on it. The results of the experimentation shows that the important parameters of surface roughness, pressure, mechanical and heat properties have effect on thermal contact resistance. The investigation presented here also states that a more efficient heat transfer is obtainable; hence thermal contact resistance can be effectively lowered. The results of the paper may provide some information for those who deal with the systems in which thermal resistance is concerned, particularly thermal management of electronics.

References

[1] M. Bahrumi, J. R. Culham, M. M. Yovanorich, *Modeling thermal contact resistance: A scale analysis approach*, J. Heat Transfer **126** (2004) 896

[2] M. Bahrumi, M. M. Yovanovich, J. R. Culham, *Thermal contact resistance at low contact pressure: Effect of elastic deformation*, Int. J. Heat and Mass Transfer **48** (2005) 3284

[3] J. R. Barber, *The influence of interface thermal contact resistance on the heat transfer performance of prestressed Duplex tube*, Int. J. Heat and Mass Transfer **29** (1986) 761

[4] R. S. Cook, K. H. Token, R. L. Calkins, *A novel concept for reducing thermal contact resistance*, J. Spacecraft and Rockets, **21** (1984) 122

[5] P. Z. Cong, X. Zhang, M. Fujii, *Estimation of thermal contact resistance using ultrasonic waves*, Int. J. Thermophysics, **27** (2006)171

[6] M. Gavarella, L. Johnssen, L. Afferante, A. Klarbin, J. R. Barber, *Interaction of thermal contract resistance and frictional heating in thermoelastic instability*, Int. J. Solids and Structures **40** (2003) 5583

[7] A. McDonald, C. Moreau, S. Chandra, *Thermal contact resistance between plasma-sprayed particles and flat surfaces*, Int. J. Heat and Mass Transfer **50** (2007) 1737

[8] K. Mizuhara, N. Ozawa, *Estimation of thermal contact resistance based on electrical contact resistance measurements*, Int. J. Japanese Society of Precision Engineering **33** (1999) 59
[9] Lecture notes on thermal contact resistance, Massachusetts Institute of Technology (MIT), open courseware, www.ocw.mit.edu/ (2007)
[10] R. K. Rajput, *Heat and mass transfer*, S. Chand & Co. Ltd, New Delhi (1998) pp. 580
[11] S. Shinji, K. Kazuhiro, S. Haruhusa, T. Kenji, *Quantitative measuring method of thermal contact resistance considered real contact area*, J. Japan Society for Precision Engineering **71** (2005) 1026
[12] B. Vermeersch, G. DeMery, *Influence of thermal contact resistance on thermal impedance of microelectronic structures*, Microelectronics Reliability **47** (2007) 1233
[13] Y. C. Yang, *Estimation of thermal contact resistance and thermally induced optical effects in single-coated optical fibers*, Optics Communications **278** (2007) 81